Contribution to modeling hydrogen permeation and barrier layer optimization in blow molded plastic liners for an on-board compressed hydrogen tanks

Benrabah, Zohir; Bardetti, Anna; Ilinca, Florin; Bournival, Sylvain

Publisher's version / Version de l'éditeur:

23rd World Hydrogen Energy Conference, 2022-06-26

Contribution to Modeling Hydrogen Permeation and Barrier Layer Optimization in Blow Molded Plastic Liners for an On-Board Compressed Hydrogen Tanks

Zohir Benrabah, Anna Bardetti, Florin Ilinca, Sylvain Bournival*
National Research Council Canada – Automotive and Surface Transportation
75 de Mortagne Blvd., Boucherville, QC J4B 6Y4, Canada

*Corresponding author e-mail: zohir.benrabah@cnrc-nrc.gc.ca;

ABSTRACT

Blow Molded Plastic Liners (BMPL) for on-board type IV Compressed Gaseous Hydrogen (CGH2) storage tanks consist of a high-molecular-weight polymer wall that serves as a permeation layer for hydrogen gas. This paper presents the latest numerical model integrated in the BlowView[1] software for predicting the hydrogen permeation in a BMPL. The prediction model is based on Fick's solution-diffusion laws, with pressure and temperature dependent transport properties, for steady/unsteady state permeation regimes through a polymeric wall. An overview of key simulation results for an industrial BMPL for a CGH2 tank, as well as the adopted methodology addressing the challenge to maximize the enclosed volume, while optimizing the wall thickness for light weighting and permeability performance, are also presented.

Keywords: type IV hydrogen tank, hydrogen permeation, plastic liner, simulation, fuel cell electrical vehicle (FCEV).

INTRODUCTION

A key challenge to the widespread commercialization of FCEV, is to design compact and cost effective on-board CGH2 tanks which store sufficient quantities of H2 without sacrificing passenger and cargo space. The first generation of FCEVs use 700 bar Type IV pressure vessels to store hydrogen [1]. These vessels have a cylindrical BMPL, overwrapped by carbon-fiber composite material to maintain the internal pressure, which serves as a hydrogen gas permeation layer. However, due to its small molecular size, H2 permeates through the plastic liner wall. This represents a serious issue that should be addressed early in the design stage in order to minimize H2 emissions from the liner and conform to legal safety requirements and standards. Meanwhile, automotive OEMs and their suppliers are being challenged to design longer and thinner liners with very consistent wall thickness. One way to meet the hydrogen permeation rate requires a judicious choice of liner material. In the thermoplastic forming industry, it is still common practice to rely on trial and error to find the appropriate barrier layer configuration/thickness required to meet the permeation rate limit requirement. A tool offering a more efficient alternative, based on reliable predictive/virtual analysis of the H2 diffusion through the BMPL wall, could significantly shorten the design/development cycle by allowing product prototypes to be analyzed and tested virtually. A finite element based model that could help a designer better understand barrier layer properties was integrated in the latest version of NRC's BlowView software [2, 3]. The mathematical diffusion model adopted is based on Fick's diffusion law to predict H2 diffusion through a polymeric wall. The resulting results, in terms of H2 permeation rate on an industrial BMPL, are presented in this work.

THE PERMEATION MECHANISM AND MATHEMATICAL MODEL

The permeation mechanism occurs in three main phases: The first phase is the absorption of the permeant (H2) into the polymer that occurs at the upstream side of the polymer wall. The second phase is the diffusion of the permeant from the surface to the core of the polymer due to the concentration gradient. Finally, the permeant desorbs on the downstream side of the membrane and is removed from the surface by convection to the surrounding air. Given the inherently low diffusivity of plastics and the special geometrical configuration of a BMPL, which is relatively thin compared to their surface area, one dimensional diffusion is usually assumed though the thickness. The permeant diffusion equation for a diffusivity, D, is given by the following expression of Fick's second law [4]:

$$\frac{\partial C}{\partial t} = -\frac{\partial}{\partial x}(J_{H2}) = -\frac{\partial}{\partial x}\left(D\frac{\partial C}{\partial x}\right) \quad (1)$$

Where, C is the permeant concentration in the polymer matrix, t is the time, and x the distance through the thickness. However, since the measurement of concentrations is not always a simple task, we instead use Henry's law, Eq. (2), where S is Henry's solubility coefficient and p_{H2} is the H2 pressure:

[1]BlowView is an engineering simulation software developed at NRC and used to simulate and optimize several forming processes: conventional, twin sheet and 3D extrusion blow molding, thermoforming and injection stretch blow molding.

$$C = S \cdot p_{H2} \quad (2)$$

The new partial differential equation (PDE) is obtained by substituting Eq. (2) in Eq. (1) as follows:

$$\frac{\partial}{\partial t}(S \cdot p_{H2}) = -\frac{\partial}{\partial x}\left(D \frac{\partial}{\partial x}(S \cdot p_{H2})\right) \quad (3)$$

EFFECT OF TEMPERATURE AND PRESSURE ON TRANSPORT COEFFICIENTS

Many references exploring the influence of temperature on the gas solubility coefficient S, diffusion coefficient D, and permeability coefficient P, in polymers have proved that the variation of the coefficients obeys an Arrhenius-type relationship over a small temperature range as [4]:

$$S = S_\infty \cdot \exp\left(-\frac{\Delta H_s}{R \cdot T}\right); \qquad D = D_\infty \cdot \exp\left(-\frac{E_D}{R \cdot T}\right); \qquad P = P_\infty \cdot \exp\left(-\frac{E_P}{R \cdot T}\right) \quad (4)$$

Where, S_∞, D_∞ and P_∞ represent the limit values of various transport coefficients when the temperature tends to infinity. ΔH_s, E_D and E_P represent the heat of dissolution required for the penetrant to dissolve in the polymer matrix, the activation energy diffusion process, and the apparent activation energy for permeation, respectively. It is obvious from the relationship $P = S \times D$ that $E_P = \Delta H_s + E_D$. For hydrogen, both ΔH_s and E_D are positive values [4]. R and T denote the universal gas constant and the absolute temperature. In general, this temperature dependence, Eq.(4), is obeyed for polymer materials at low pressures as long as the microstructure of the material is not changing. On the other hand, high pressures will affect the microstructure, and therefore, the permeation depends on the imposed stresses and material characteristics. The polymer transport properties will be considered for ideal sorption where the effects of hydrostatic pressure on the polymeric structure can be idealized as arising from two opposing effects: (1) the compression of the polymer due to imposed hydrostatic pressure, which reduces diffusion (negative β_D); and (2) the swelling of the polymer due to hydrogen solubility, which enhances diffusion (positive β_s) [5].. These two effects are combined in a single parameter β as described in equation (5).

$$S = S_0 \cdot \exp(\beta_s \cdot p_{H2}); \qquad D = D_0 \cdot \exp(\beta_D \cdot p_{H2}); \qquad P = P_0 \cdot \exp((\beta_s + \beta_D) \cdot p_{H2}) \quad (5)$$

Where, S_0, D_0 and P_0 represent values of various transportation coefficients at atmospheric pressure and $\beta = \beta_s + \beta_D$. Therefore, the combined effect of the temperature and pressure on the transport coefficients can be obtained by substituting Eq.(4) in Eq.(5):

$$S = S_\infty \cdot exp\left(\beta_s \cdot p_{H2} - \frac{\Delta H_s}{R \cdot T}\right); \qquad D = D_\infty \cdot exp\left(\beta_D \cdot p_{H2} - \frac{E_D}{R \cdot T}\right); \qquad P = P_\infty \cdot exp\left((\beta_s + \beta_D) \cdot p_{H2} - \frac{\Delta H_s + E_D}{R \cdot T}\right) \quad (6)$$

NUMERICAL RESOLUTION

After substituting the solubility and diffusivity expression from Eq.(6) in Eq.(3) we obtain the following PDE:

$$\frac{\partial}{\partial t}\left(S_\infty \cdot \exp\left(\beta_s \cdot p_{H2} - \frac{\Delta H_s}{R \cdot T}\right) \cdot p_{H2}\right) + \frac{\partial}{\partial x}\left(D_\infty \cdot \exp\left(\beta_D \cdot p_{H2} - \frac{E_D}{R \cdot T}\right) \frac{\partial}{\partial x}\left(S_\infty \cdot \exp\left(\beta_s \cdot p_{H2} - \frac{\Delta H_s}{R \cdot T}\right) \cdot p_{H2}\right)\right) = 0 \quad (7)$$

An appropriate numerical method is used to solve the obtained transient nonlinear PDE with respect to the initial boundary conditions. The finite element method is used for space discretization and the Euler implicit scheme for time integration. Details regarding the mathematical formulation of the space discretization and the time integration are not provided here since they fall out of the scoop of this work.

PLASTIC LINER SIMULATION RESULTS

The H2 permeation rate for a typical BMPL was predicted using BlowView for different permeation scenarios and the results are presented below. The length and the diameter of the industrial liner are 365 and 720 mm, respectively. The corresponding enclosed volume capacity is 62.4L. Figures 1a and 1b show the predicted thickness distribution at the end of parison extrusion, inflation and finally after mapping, for the initial and optimized design. The liner weight was reduced from 10.6 kg to 10.3 kg after 19 optimization iterations by improving the thickness uniformity. It is important to note that the permeability analysis was performed on the optimized mapped part, with the H2 stored at a constant pressure of 70 MPa. The temperature and pressure dependent H2 solubility and diffusivity coefficients for three HDPE grades are reported in Table 1 [4, 5]. Figure 2 illustrates the predicted H2 flux over the monolayer liner shell for the different HDPE grades at 20°C. The overall H2 permeation is also reported and should be compared to the maximum allowable limit at 20°C and 45°C provided by [6]. From Figure 2.a, we notice that the H2 permeation of the HDPE-1 liner (i.e., 17.2 NmL/hr/L) exceeds the maximum allowable limit at 20°C (i.e., 8.0 NmL/hr/L). However, as illustrated in Figures 2.b and 2.c, the permeation of the liners made from materials HDPE-2 and HDPE-3 are, respectively, 5.1 and 3.5

NmL/hr/L, both below the maximum allowable. From Figure 2.d, we also observe that the H2 permeation for HDPE-3 increases to 26.4 NmL/hr/L at 45°C, which represents +700% compared to 20°C. Unfortunately, we can't compare this result to the maximum allowable permeation rate at 45°C since this information is not available in the literature.

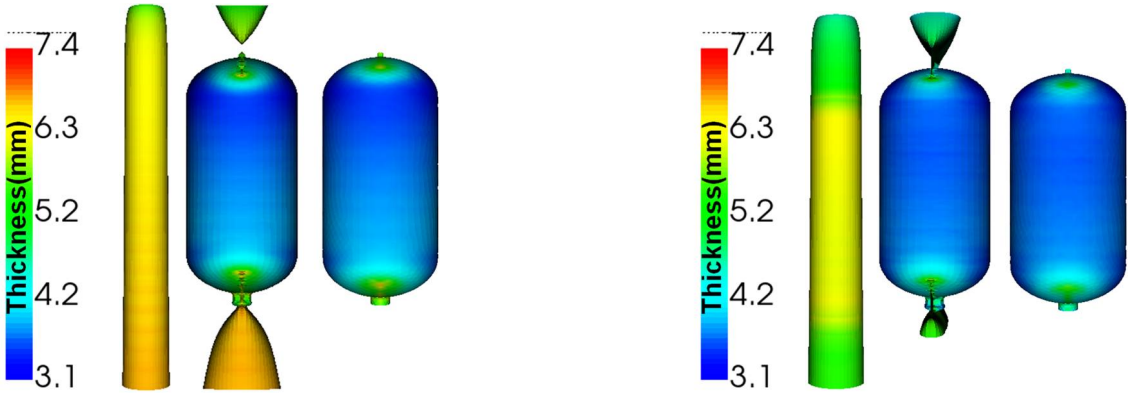

a: Initial design (6.6 kg) b: Optimized design (6.3 Kg)

Figure 1: BlowView predicted thickness distribution

Table 1: H2 solubility and diffusivity coefficients for 3 different HDPE grades

Diffusivity	D_∞(m^2/s)	$E_D(J/molH2)$	β_D(MPa-1)	**Solubility**	S_∞(mol H2/m^3/MPa)	$\Delta H_S(J/molH2)$	β_S(MPa-1)
HDPE-1	0.0970	48837.0	0.0	HDPE-1	0.097	48837.0	0.0
HDPE-2	0.0970	48837.0	-0.05	HDPE-2	0.097	48837.0	0.003
HDPE-3	0.0970	48837.0	-0.07	HDPE-3	0.097	48837.0	0.003

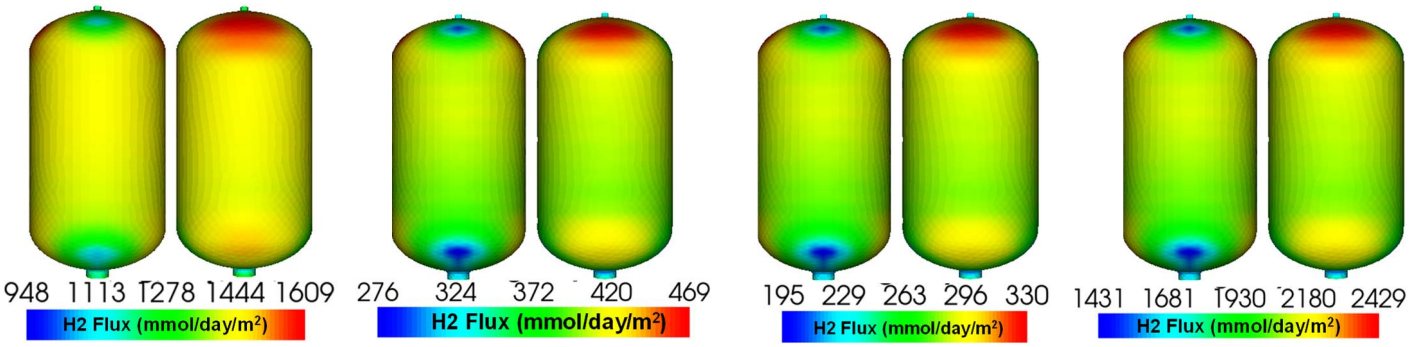

a: HDPE-1 (pressure independent) 17.2 NmL/hr/L at 20°C

b: HDPE-2 5.1 NmL/hr/L at 20°C

c: HDPE-3 3.5 NmL/hr/L at 20°C

d: HDPE-3 26.4 NmL/hr/L at 45°C

Figure 2: Hydrogen permeation and flux density for 3 different HDPE grades

CONCLUSIONS

A finite element based numerical simulation model for the prediction of H2 permeation through a BMPL for a CGH2 storage tank in steady and unsteady regimes, incorporating a novel method for the treatment of the diffusion in the pinch-off zone, was developed. This H2 permeation model was incorporated in BlowView to optimize the barrier layer to satisfy the daily permeation rate constraint. More results will be shared during the conference presentation.

REFERENCES

1. Johnson, K., Veenstra, M., Gotthold, D., Simmons, K. et al., SAE Int. J. Alt. Power. 6(2):2017.
2. Benrabah Z., Thibault P., DiRaddo R., SAE Transactions Journal of Fuel and Lubricants, V 115, 4, pp219-226, 2006.
3. Benrabah Z., Thibault P., DiRaddo R., SAE International Journal of Materials and Manufacturing, pp. 449-459, 2011.
4. Neogi, P., Transport Phenomena in Polymer Membranes, New York: Marcel Dekker, (1996).
5. Barth R. R., Simmons K. L., Marchi C. S., Polymers for Hydrogen Infrastructure and Vehicle Fuel Systems:Applications, Properties, and Gap Analysis, Sandia Report, SAND2013-8904, October 2013
6. Adams P., Bengaouer A., Cariteau B., Molkov V., Venetsanos A.G., Allowable hydrogen permeation rate from road vehicles, int. jour. of hydrogen energy 36 (2011) 2742-2749